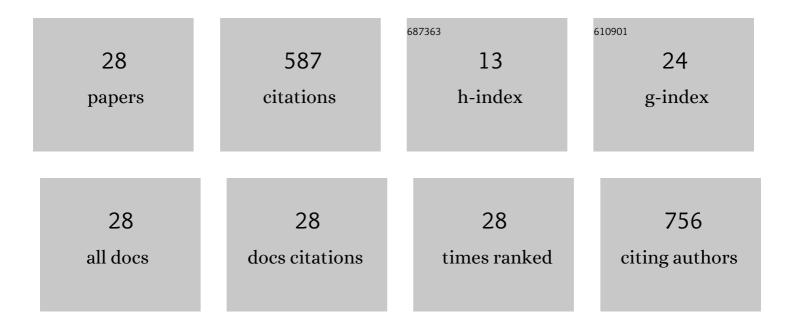
## Hongping Li

List of Publications by Year in descending order

Source: https://exaly.com/author-pdf/8584212/publications.pdf Version: 2024-02-01



HONCRINCLI

#	Article	IF	CITATIONS
1	Passivation functionalized phenothiazine-based hole transport material for highly efficient perovskite solar cell with efficiency exceeding 22%. Chemical Engineering Journal, 2021, 410, 128328.	12.7	83
2	Highly efficient phenothiazine 5,5-dioxide-based hole transport materials for planar perovskite solar cells with a PCE exceeding 20%. Journal of Materials Chemistry A, 2019, 7, 9510-9516.	10.3	60
3	Electrical conductivity optimization in electrolyte-free fuel cells by single-component Ce0.8Sm0.2O2-δ〓Li0.15Ni0.45Zn0.4 layer. RSC Advances, 2012, 2, 3828.	3.6	57
4	<i>A</i> -Site-Doping Enhanced <i>B</i> -Site Ordering and Correlated Magnetic Property in La <sub>2–<i>x</i></sub> Bi <sub><i>x</i></sub> CoMnO <sub>6</sub> . Journal of Physical Chemistry C, 2012, 116, 16841-16847.	3.1	46
5	Highly Efficient Phenoxazine Core Unit Based Hole Transport Materials for Hysteresis-Free Perovskite Solar Cells. ACS Applied Materials & Interfaces, 2018, 10, 36608-36614.	8.0	41
6	Molecular Engineering of Triphenylamine-Based Non-Fullerene Electron-Transport Materials for Efficient Rigid and Flexible Perovskite Solar Cells. ACS Applied Materials & Interfaces, 2018, 10, 38970-38977.	8.0	34
7	Cyclic Compound Formation Mechanisms during Pyrolysis of Typical Aliphatic Acidic Amino Acids. ACS Sustainable Chemistry and Engineering, 2020, 8, 16968-16978.	6.7	32
8	Highly efficient perovskite solar cells based on symmetric hole transport material constructed with indaceno[1,2-b:5,6-b']dithiophene core building block. Journal of Energy Chemistry, 2020, 43, 98-103.	12.9	31
9	Direct Determination of Atomic Structure and Magnetic Coupling of Magnetite Twin Boundaries. ACS Nano, 2018, 12, 2662-2668.	14.6	30
10	Insight into the Mechanism of Glycerol Dehydration and Subsequent Pyridine Synthesis. ACS Sustainable Chemistry and Engineering, 2021, 9, 3095-3103.	6.7	23
11	Strain control of orbital polarization and correlated metal-insulator transition in La2CoMnO6 from first principles. Applied Physics Letters, 2011, 99, .	3.3	21
12	Mechanism of A-B intersite charge transfer and negative thermal expansion in A-site-ordered perovskite LaCu3Fe4O12. Journal of Applied Physics, 2012, 111, 103718.	2.5	17
13	Fluorineâ€Substituted Benzotriazole Core Building Blockâ€Based Highly Efficient Holeâ€Transporting Materials for Mesoporous Perovskite Solar Cells. Solar Rrl, 2020, 4, 1900362.	5.8	16
14	Facile synthesized fluorine substituted benzothiadiazole based dopant-free hole transport material for high efficiency perovskite solar cell. Dyes and Pigments, 2021, 184, 108786.	3.7	15
15	<i>B</i> -site ordering induced suppression of magnetic cluster glass and dielectric anomaly in La2â°' <i>x</i> Bi <i>x</i> CoMnO6. Applied Physics Letters, 2012, 100, .	3.3	11
16	Covalent State and the Electronic and Transport Properties of CaCu <sub>3</sub> Ni <sub>4</sub> O <sub>12</sub> : A First-Principles Study. Journal of Physical Chemistry C, 2011, 115, 2366-2370.	3.1	10
17	Firstâ€principles investigation of Aâ€B intersite charge transfer and correlated electrical and magnetic properties in BiCu <sub>3</sub> Fe <sub>4</sub> O <sub>12</sub> . Journal of Computational Chemistry, 2011, 32, 1235-1240.	3.3	10
18	First-principles study of negative thermal expansion mechanism in A-site-ordered perovskite SrCu <sub>3</sub> Fe <sub>4</sub> O <sub>12</sub> . RSC Advances, 2015, 5, 1801-1807.	3.6	10

Hongping Li

#	Article	IF	CITATIONS
19	Study on the pyrolysis mechanism of unsaturated fatty acid: A combined density functional theory and experimental study. International Journal of Energy Research, 2022, 46, 2029-2040.	4.5	10
20	Ferrimagnetic semiconductor with a direct bandgap. Applied Physics Letters, 2020, 116, .	3.3	7
21	Spin Polarization-Assisted Dopant Segregation at a Coherent Phase Boundary. ACS Nano, 2021, 15, 19938-19944.	14.6	6
22	Unraveling the effect of B-site antisite defects on the electronic and magnetic properties of the quadruple perovskite CaCu <sub>3</sub> Fe <sub>2</sub> Nb <sub>2</sub> O <sub>12</sub> . Physical Chemistry Chemical Physics, 2019, 21, 3059-3065.	2.8	5
23	Firstâ€principle investigation of magnetic coupling mechanism in hypothesized Aâ€siteâ€ordered perovskite YMn <sub>3</sub> Sc <sub>4</sub> O <sub>12</sub> . Journal of Computational Chemistry, 2012, 33, 82-87.	3.3	4
24	Benzo[1,2- <i>c</i> :4,5- <i>c</i> ′]dithiophene-4,8-dione (BDD) Core Building Block Based Dopant-Free Hole-Transport Materials for Efficient and Stable Perovskite Solar Cell. ACS Applied Energy Materials, 2020, 3, 10333-10339.	5.1	3
25	The peculiar magnetic property evolution along RCu3Mn4O12 (R=Y, La, Pr, Nd, Sm, Eu, Gd, Tb, Dy, Ho, Er,) Tj ETC	2q110.78	4314 rgBT
26	The impact of B-site antisite defects on the magnetic and electronic properties in double perovskite Pb2FeOsO6. Ceramics International, 2021, 47, 992-1001.	4.8	2
27	A half-metallic ferrimagnet of CeCu3Cr4O12 with 4f itinerant electron. Applied Physics Letters, 2020, 117, 132404.	3.3	1
28	Ferrimagnetic semiconductor of CaCu3Fe2V2O12 with direct bandgap. Chemical Physics Letters, 2020, 759, 137910.	2.6	0